Improved Therapeutic Responses in a Xenograft Model of Human B Lymphoma (Namalwa) for Liposomal Vincristine *versus* Liposomal Doxorubicin Targeted via Anti-CD19 IgG2a or Fab′ Fragments

Puja Sapra, Elaine H. Moase, Jie Ma, and Theresa M. Allen

Department of Pharmacology, University of Alberta, Edmonton, Alberta, Canada

ABSTRACT

Purpose: **Monoclonal antibody-mediated targeting of liposomal anticancer drugs to surface antigens expressed on malignant B cells can be an effective strategy for treating B-cell malignancies. In a murine model of human B-cell lymphoma, we have made *in vitro* and *in vivo* comparisons of long-circulating sterically stabilized (Stealth) immunoliposome (SIL) formulations of two anticancer drugs, vincristine (VCR) and doxorubicin (DXR), with different mechanisms of action and drug release rates.**

Experimental Design: **SIL formulations of VCR or DXR were conjugated to the monoclonal antibody anti-CD19 (SIL[αCD19]) or its Fab′ fragments (SIL[Fab′]). Specific binding of SILs to Namalwa cells was studied using radiolabeled liposomes, and cytotoxicities of DXR- or VCR-loaded SILs were quantitated by a tetrazolium assay. Pharmacokinetic and drug leakage experiments were performed in mice using dual-labeled liposomes, and the therapeutic responses of SILs were evaluated in a Namalwa (human B lymphoma) cell xenograft model.**

Results: **SIL[αCD19] or SIL[Fab′] had higher association with and cytotoxicity against Namalwa cells than nontargeted liposomes. SIL[Fab′] had longer circulation times than SIL[αCD19], and VCR had faster release rates from the liposomes than DXR. SIL formulations of either VCR or DXR had significantly better therapeutic outcomes than nontargeted liposomes or free drugs. SILs loaded with VCR were superior to those loaded with DXR. SIL[Fab′] had better therapeutic outcomes than SIL[αCD19] for the drug DXR but were equally efficacious for the drug VCR.**

Conclusions: **Treatment of a B lymphoma model with single injections of anti-CD19-targeted liposomal formulations of VCR resulted in high levels of response and long-term survivors. Responses to anti-CD19-targeted liposomal DXR were more modest, although the longer circulation times of SIL[Fab′] *versus* SIL[αCD19] led to superior therapeutics for DXR-loaded immunoliposomes.**

INTRODUCTION

Anticancer chemotherapy is compromised by dose-limiting side effects as a consequence of the distribution of anticancer drugs to normal cells and tissues as well as to malignant ones. Trapping cytotoxic drugs in liposomes can reduce their side effects as well as improve their therapeutic effectiveness by enhancing their localization to tissues with increased vascular permeability, *e.g.*, solid tumors undergoing angiogenesis (1, 2). This approach, referred to as passive targeting, has resulted in several liposomal anticancer drugs that have received clinical approval and many more that are in clinical trials.

There is currently increased interest in the use of ligand-mediated or "active" targeting as a strategy for increasing the therapeutic effectiveness of antineoplastic drugs. To form targeted liposomes, monoclonal antibodies (mAbs), peptides, or growth factors that bind selectively to tumor-associated surface antigens or receptors are coupled to the liposome surface (3–12). Antibodies or antibody fragments that are capable of inducing efficient receptor-mediated internalization of immunoliposomes can result in significant increases in the amount of drug delivered to the target cells and enhanced therapeutic outcomes relative to free drugs, noninternalizing antibodies, or nontargeted liposomes (13–15). In addition, many mAbs have unique signaling properties, such as inhibition of DNA repair (16), blockade of P-glycoprotein (17), or induction of apoptosis (18), that lead to anticancer effects that may synergize with the cytotoxic effects of liposomal anticancer drugs (19–21).

Despite the observation that immunoliposomes improve the therapeutic effectiveness of anticancer drugs, some further development is required before clinical testing. One of the most widely used antibody coupling techniques for the preparation of immunoliposomes relies on thiolation of amino residues on whole IgG antibody molecules (22). Such modifications can alter the biological activity of the antibody molecule, *e.g.*, by randomly thiolating the active site, which can result in interference with either the binding of the antibody to its receptor or receptor activation and/or receptor internalization.

The immunogenicity of therapeutic agents that are based on murine mAbs has been a major barrier to successful therapy in humans because they evoke human antimouse antibodies, mediated in part by the Fc region of the molecule (23–25). This

Received 8/14/03; revised 10/21/03; accepted 10/28/03.
Grant support: Canadian Institutes of Health Research Grant MOP-9127.
The costs of publication of this article were defrayed in part by the payment of page charges. This article must therefore be hereby marked *advertisement* in accordance with 18 U.S.C. Section 1734 solely to indicate this fact.
Notes: Present address for Jie Ma is State Key Laboratory of Molecular Oncology, Cancer Institute, Chinese Academy of Medical Sciences, PUMC, Panjiayuan, Beijing, 100021 People's Republic of China. Puja Sapra is a recipient of a University of Alberta, F. S. Chia Ph.D. Scholarship and an Alberta Heritage Foundation for Medical Research Studentship.
Requests for reprints: Theresa M. Allen, Department of Pharmacology, University of Alberta, Edmonton, Alberta, T6G 2H7 Canada. Phone: (780) 492-5710; Fax: (780) 492-8078; E-mail: terry.allen@ualberta.ca.

can result in hypersensitivity reactions and, in the case of immunoliposomes, enhanced removal of the immunoliposomes by the cells of the mononuclear phagocyte system via Fc receptors on macrophages (26–28). Because the extent of uptake of liposomes by target tissues is directly related to their residence time in the circulation, any decrease in the circulation half-lives of liposomes due to nonspecific uptake mechanisms will compromise their selective uptake by the target tissues (29). Furthermore, some studies have reported that targeted liposomes containing exposed Fc regions of the antibody are taken up by tumor-associated macrophages, which limits their direct interactions with the target tumor cells (5, 30, 31).

Antibody fragments that contain the relevant antigen binding site, *e.g.*, Fab′ or scFv fragments, are attractive alternatives to whole mAbs as liposomal targeting agents. Fab′ fragments can be coupled to liposomes through the thiol groups of the hinge region, avoiding perturbation of the antigen recognition site and introduction of random amino acid modifications to the antibody (32, 33). Removal of the Fc domain helps liposomes evade uptake by the Fc receptors on macrophages and should reduce immunogenicity of the immunoliposomes. It will also increase their circulation times and therefore increase the degree of tumor localization of the immunoliposomes (6, 34). Although binding avidity is lost with the use of univalent Fab′ and scFv fragments, coupling of these fragments to liposomes will restore multivalency and binding avidity.

The *Vinca* alkaloid vincristine (VCR) is used in the treatment of lymphomas. It is a cell cycle-dependent drug that arrests cell mitosis during metaphase by preventing tubulin polymerization as well as by inducing depolymerization. However, dose-limiting toxicities such as peripheral neuropathy associated with VCR therapy can compromise both the therapeutic outcome and patient quality of life. *In vitro* studies have demonstrated a positive relationship between the therapeutic efficacy of VCR and the length of exposure of tumor cells to the drug (35). A nonpegylated liposomal formulation of VCR is currently in clinical trials (36, 37). The use of a mAb-targeted, long-circulating liposomal formulation of VCR should increase the amount of drug delivered to the target cells and increase the duration of exposure of the target cells to the drug, both of which should result in an improved therapeutic outcome. The exposure of sensitive tissues to the drug will be decreased, leading to reduced side effects.

The ability of liposome-encapsulated doxorubicin (DXR) to decrease the side effects of the drug and to increase its therapeutic effectiveness is well established in the clinic (38–40). The utility of liposomal DXR targeted via whole murine anti-CD19 antibodies has been described previously in our laboratory in severe combined immunodeficient (SCID) mouse models of human B lymphoma and multiple myeloma (7, 41). A comparison of Fab′-targeted liposomal DXR with whole mAb-targeted liposomal DXR would allow us to test the hypothesis that Fab′-targeted liposomes will have therapeutic advantages, in part due to their pharmacokinetic advantages.

In this study, we evaluated the binding, cytotoxicity, pharmacokinetics, and therapeutic outcomes for anti-CD19-targeted liposomal formulations of two different cytotoxic drugs, VCR and DXR, which act via different mechanisms of action and have different drug-related properties and different drug release rates from liposomes. We compared the therapeutic responses, in a SCID mouse model of human B-cell lymphoma, of liposomal drugs targeted with whole mAb or Fab′ molecules, with results obtained for free drugs or drug-loaded, nontargeted liposomes. Antibody-targeted liposomal drugs resulted in significant improvements in therapeutic responses compared with other treatment groups. Single i.v. injections of antibody-targeted liposomal VCR, at one-third of the maximum tolerated dose (MTD), resulted in long-term survivors and were superior to antibody-targeted liposomal DXR.

MATERIALS AND METHODS

Chemicals. Egg sphingomyelin (SM) and cholesterol (Chol) were purchased from Avanti Polar Lipids (Alabaster, AL). Methoxypoly(ethylene glycol) (M_r 2000), covalently linked via a carbamate bond to distearoylphosphatidylethanolamine (mPEG-DSPE; Ref. 42), hydrogenated soy phosphatidylcholine (HSPC), and DXR were generous gifts from ALZA Pharmaceuticals, Inc. (Mountain View, CA). Maleimide-derivatized poly(ethylene glycol)$_{2000}$-distearoylphosphatidylethanolamine (Mal-PEG-DSPE) was custom synthesized by Shearwater Polymers, Inc. (Huntsville, AL), according to a previously described protocol (43). Nuclepore polycarbonate membranes (pore sizes, 0.2, 0.1, and 0.08 μm) were purchased from Northern Lipids (Vancouver, British Columbia, Canada). VCR sulfate (1 mg/ml) for injection was purchased from the pharmacy of the University of Alberta Hospital (Edmonton, Alberta, Canada). RPMI 1640 (without phenol red), penicillin-streptomycin, fetal bovine serum, and adult bovine serum (ABS) were purchased from Life Technologies, Inc. (Burlington, Ontario, Canada). 2-Iminothiolane (Traut's reagent), 2-mercaptoethylamine-HCl, and 3-(4,5-dimethylthiazol-2-yl)-2,5-diphenyltetrazolium bromide were obtained from Sigma Chemical Co. (St. Louis, MO). Iodobeads, protein A/G column, Immuno-Pure IgG elution buffer, Slide-A-Lyzer dialysis cassettes (M_r cutoff of 10,000), and buoys were purchased from Pierce (Rockford, IL). Lysyl endopeptidase enzyme was obtained from Wako Chemicals Inc. (Richmond, VA). SDS-PAGE gels (4–20% acrylamide, Tris-HCl buffer system) and Bio-Rad Protein Assay Reagent were purchased from Bio-Rad Laboratories (Mississauga, Ontario, Canada). Sephadex G-25 and G-50, Sepharose CL-4B, aqueous counting scintillant, [^{3}H]VCR (1.85 MBq), and [^{14}C]DXR (185 KBq) were purchased from Amersham Pharmacia Biotech (Baie d'Urfe, Quebec, Canada). [^{14}C]VCR was a kind gift from Inex Pharmaceuticals (Vancouver, British Columbia, Canada). Chol-[1,2-^{3}H-(*N*)]hexadecyl ether ([^{3}H]CHE; 1.48–2.22 TBq/mmol), Solvable, and Ultima Gold were purchased from Perkin-Elmer Biosciences (Boston, MA). Centrisart concentrators (M_r cutoff of 100,000) were obtained from Sartorius (Gottingen, Germany), and Microcon YM-10 concentrators were from Millipore Corp. (Bedford, MA). All other chemicals were of analytical grade purity or the highest available purity.

Animals, Tumor Cell Line, and Antibodies. Female 6–8-week-old BALB/c mice were obtained from the Health Sciences Laboratory Animal Services (University of Alberta) and kept in standard housing. Female 6–8-week old CB17 SCID mice were purchased from Taconic Farms (Germantown,

NY) and housed in the virus antigen-free unit of the Health Sciences Laboratory Animal Services, University of Alberta. All experiments were approved by the Health Sciences Animal Policy and Welfare Committee of the University of Alberta. The human Burkitt's lymphoma cell line Namalwa (ATCC CRL 1432) was purchased from American Type Culture Collection (Manassas, VA) and cultured in suspension in a humidified 37°C incubator with a 5% CO_2 atmosphere in RPMI 1640 supplemented with 10% (v/v) fetal bovine serum, penicillin G (50 units/ml), and streptomycin sulfate (50 μg/ml). For experiments, only cells in the exponential phase of cell growth were used.

The anti-CD19 murine monoclonal antibody IgG2a (αCD19) was produced from the FMC63 murine hybridoma [from Dr. H. Zola; Children's Health Research Institute, Adelaide, Australia (44)] and purified as described previously (45). An isotype-matched (IgG2a) control antibody, αPK136, was produced from the HB191 murine hybridoma (American Type Culture Collection). To prepare Fab′ fragments, mAb αCD19 was incubated with lysyl endopeptidase at a molar ratio of 1:200 (enzyme:substrate) in HEPES-buffered saline (pH 8.0) for 3 h at 37°C (46), after which the digest was chromatographed on an immobilized protein A/G column equilibrated with Tris buffer [0.1 M Tris-HCl and 0.15 M NaCl (pH 8.0)] to adsorb any undigested IgG2a and the Fc segment of the antibody. The disulfide bridges of $F(ab')_2$ thus obtained were reduced using 5 mM 2-mercaptoethylamine-HCl for 60 min at 37°C. The sample was then eluted over a Sephadex G-25 column equilibrated with degassed HBS (pH 7.4) to remove free 2-mercaptoethylamine-HCl. Fab′ fragments were maintained in an O_2-free environment. Protein concentrations were determined by the Bio-Rad Protein Assay, and the preparation of $F(ab')_2$ and Fab′ fragments was confirmed by SDS-PAGE analysis. The molecular weights of the $F(ab')_2$ and Fab′ fragments of αCD19 were approximately 110,000 and 55,000, respectively and the final recovery of Fab′ fragments was 50–60%. Fab′ fragments of the isotype-matched control antibody (αPK136) were prepared by the same protocol.

Preparation of Liposomes. Nontargeted liposomes to be loaded with VCR were composed of SM:Chol:mPEG-DSPE at a 55:40:5 molar ratio [Stealth liposomes composed of SM:Chol:mPEG-DSPE (SM-SL)] and were similar to previously described VCR formulations, except that mPEG-DSPE was included in the lipid bilayer (35). VCR was encapsulated by a transmembrane pH gradient-dependent procedure as described previously (47). In some cases, radiolabeled [^{3}H]VCR sulfate (5 μCi [^{3}H]VCR sulfate/mg unlabeled VCR) was added as a radioactive tracer. Targeted liposomes (see below) were composed of SM:Chol:mPEG-DSPE:Mal-PEG-DSPE, at a 55:40:4:1 molar ratio (SM-SIL). The dried lipid film was hydrated in 300 mM citrate buffer (pH 4.0) with occasional vortexing and heating at 65°C to give a concentration of 25–30 mM phospholipid (PL). The liposomes were then sequentially extruded (Lipex Biomembranes Extruder, Vancouver, British Columbia, Canada) through a series of polycarbonate membranes with pore sizes of 0.2, 0.1, and 0.08 μm to achieve a final size of 120–130 nm. The liposome particle size was analyzed using a Brookhaven BI90 submicron particle sizer (Brookhaven Instruments Corp., Holtsville, NY). VCR entrapment was determined either by spectrophotometry ($\lambda = 297$ nm) in ethanol:water (8:2 by volume) or from the specific activity counts of [^{3}H]VCR or [^{14}C]VCR tracers (Beckman LS-6800 Scintillation Counter). PL concentration was determined using the Barlett colorimetric assay (48) or from the specific activity of the [^{3}H]CHE tracer (Beckman LS-6800 Scintillation Counter). Loading efficiency was determined from the drug:lipid ratio before and after encapsulation of the drug. Trapping efficiencies of ≥95% could routinely be achieved by this procedure. In some cases, the liposomes were concentrated using Centrisart concentrators.

Nontargeted liposomes to be loaded with DXR were composed of HSPC:Chol:mPEG-DSPE at a 2:1:0.10 molar ratio [Stealth liposomes composed of HSPC:Chol:mPEG-DSPE (HSPC-SL)], and targeted liposomes (see below) were composed of HSPC:Chol:mPEG-DSPE:Mal-PEG-DSPE at a 2:1:0.08:0.02 molar ratio (HSPC-SIL). They were prepared by hydration of thin films, as described previously, and extruded to a mean diameter of 100 ± 10 nm (14). DXR was loaded into liposomes using the ammonium sulfate loading method of Bolotin *et al.* (7, 49).

Coupling of Immunoliposomes. αCD19 mAb or Fab′ fragments of αCD19 were coupled to the terminus of the Mal-PEG-DSPE coupling lipid included in SM-SIL or HSPC-SIL at 2000:1 or 1000:1 (lipid:protein) molar ratios, respectively, using the coupling procedure described previously (43). These ratios were selected to provide comparable numbers of CD19 binding sites on the immunoliposomes, bearing in mind that IgG2a has two binding sites, and Fab′ has only one. For coupling of the whole antibody, to give sterically stabilized (Stealth) immunoliposomes (SILs) composed of HSPC:Chol:mPEG-DSPE conjugated to αCD19 (HSPC-SIL[αCD19]) or SILs composed of SM:Chol:mPEG-DSPE conjugated to αCD19 (SM-SIL[αCD19]), the protocol was as described previously (45). For Fab′-coupled liposomes [SILs composed of HSPC:Chol:mPEG-DSPE conjugated to Fab′ (HSPC-SIL[Fab′]) or SILs composed of SM:Chol:mPEG-DSPE conjugated to Fab′ (SM-SIL[Fab′])], the Fab′ fragments were generated from $F(ab')_2$ immediately before coupling; they were then incubated with HSPC-SIL or SM-SIL in an oxygen-free environment overnight with continuous stirring. Coupling efficiency was determined from the ratio of nmol protein/μmol PL, before and after coupling. Coupling of Fab′ fragments was assessed by adding a trace amount of ^{125}I-labeled $F(ab')_2$ at the time of cleavage with 2-mercaptoethylamine-HCl. To assess coupling of whole antibody, a trace amount of ^{125}I-labeled αCD19 was added to the unlabeled antibody before thiolation. A coupling efficiency of 80–90% for αCD19 and 50–70% for Fab′ could routinely be achieved by this procedure. αPK136, an isotype-matched, nonspecific control antibody, or its Fab′ fragments were coupled to the liposomes in a similar fashion [SILs composed of SM:Chol:mPEG-DSPE conjugated to an isotype-matched control antibody anti-PK136 IgG2a (SM-SIL[NS-Ab]) and SILs composed of SM:Chol:mPEG-DSPE conjugated to Fab′ fragments of an isotype-matched control antibody anti-PK136 (SM-SIL[NS-Fab′])].

Binding and Cytotoxicity of Immunoliposomes. *In vitro* cell association of immunoliposomes labeled with [^{3}H]CHE (nonmetabolizable, nonexchangeable radioactive tracer) was determined, as described previously, at both 37°C

and 4°C, *i.e.*, permissive and nonpermissive temperatures for endocytosis, respectively (7). Liposome uptake (pmol PL uptake/10^6 Namalwa cells) was calculated from the specific activity of the liposomes. Nonspecific binding was determined for the corresponding radiolabeled liposomes coupled to the isotype-matched control antibody, αPK136. Specific binding was determined by subtracting nonspecific binding from the total binding. The maximum number of binding sites/cell (B_{max}) and the dissociation constant (K_d) values were determined by nonlinear regression using GraphPad Prism software (San Diego, CA).

The *in vitro* cytotoxicities of free VCR, free DXR, and various liposomal formulations of VCR or DXR were determined using the 3-(4,5-dimethylthiazol-2-yl)-2,5-diphenyltetrazolium bromide dye reduction assay as described previously (7). Results are expressed as IC_{50}, which was obtained graphically using SlideWrite software (Advanced Graphics Software, Encinitas, CA).

Drug Release Rates, Pharmacokinetics, and Biodistribution. The release rate of VCR from the various liposomal formulations was determined *in vitro* in 50% ABS. Liposomes loaded with radiolabeled VCR were diluted in ABS (1:1 by volume), loaded in a dialysis cassette (M_r cutoff of 10,000), and dialyzed against 50% ABS at 37°C. At different time points, aliquots were counted for [^{3}H]VCR. The final PL concentration of all of the formulations was 0.5 mM. Results are expressed as $t_{1/2}$ (time in which 50% of drug leaks out from liposomes). Leakage of DXR has previously been determined in our laboratory to have a $t_{1/2}$ for drug release in 50% ABS of the order of 90 h, when encapsulated in liposomes of the composition used in our experiments.[1] For determining *in vivo* release rates and for pharmacokinetic and biodistribution experiments, liposomes were prepared using [^{3}H]CHE as a lipid label and either [^{14}C]VCR or [^{14}C]DXR as drug labels. Naïve BALB/c mice (3 mice/time point) received injection with liposomal formulations of the drugs at the same dose as that chosen for the therapeutic studies (0.66 mg/kg VCR or 3 mg/kg DXR). At selected time points, mice were euthanized by cervical dislocation. Whole blood was collected via cardiac puncture with a heparinized syringe, and liver and spleen were dissected out. Tissues were further processed using a method similar to those described previously (50–52). Plasma was isolated from whole blood by centrifugation at 3000 × *g* for 5 min. Liver and spleen homogenates [10% (w/v) or 5% (w/v), respectively] were prepared in water using a Polytron homogenizer (Brinkman Instruments, Mississauga, Ontario, Canada), and 500 μl of Solvable were added to 200 μl of either tissue homogenates or plasma. The solutions were then digested for 2 h at 60°C. After the vials cooled to room temperature, 50 μl of 200 mM EDTA were added before overnight bleaching with 200 μl of hydrogen peroxide [30% (v/v)]. The next day, 100 μl of 1 N HCl were added before 5 ml of Ultima Gold, and the samples were counted in a Beckman LS 6500 liquid scintillation counter for ^{3}H and ^{14}C counts.

Blood correction factors were applied to correct for liposomes present in the blood volume of organs (53). Results are expressed as percentage of injected drug or PL concentration present in blood or organs at each time point.

To provide an estimate of drug leakage *in vivo*, the ratio of either [^{14}C]VCR or [^{14}C]DXR drug counts to [^{3}H]CHE lipid counts was normalized to 1 at time 0. The rate of decrease of the drug:lipid ratio at subsequent time points indicates the rate of release of the drug from the liposomes.

***In Vivo* Survival Experiments.** SCID mice (5–7 mice/group) received i.v. injection in the tail vein with 5×10^6 Namalwa cells in 0.2 ml of PBS. Treatments with free or liposomal drugs were given 24 h later as single bolus i.v. doses of either 0.66 mg/kg VCR (approximates the human clinical dose of 2 mg/m^2) or 3 mg/kg DXR (the MTD in SCID mice). This particular dose of VCR was selected because in our previous experiments, no difference between free VCR and liposomal/immunoliposomal VCR was observed when mice were dosed at the MTD of VCR (2 mg/kg^2).[2] Mice were monitored daily and euthanized when they developed hind leg paralysis.

Statistical Analysis. Comparisons of the cellular binding and uptake, cytotoxicities, and pharmacokinetics were done using one-way ANOVA with InStat software (GraphPad software version 3.0). The Tukey post-test was used to compare means. Differences were considered significant at $P < 0.05$. K_d and B_{max} values were calculated using GraphPad Prism software. Survival studies were analyzed using Kaplan-Meier plots, with GraphPad Prism software.

RESULTS

***In Vitro* Cellular Association of Immunoliposomes.** *In vitro* cell association studies were performed to determine the targeting effectiveness of immunoliposomes to CD19$^+$ Namalwa cells. The term cell association reflects a combination of three processes: (*a*) specific binding of SILs to the CD19 epitope at the cell surface; (*b*) internalization of the SILs into the cell interior and recycling of the epitope back to the cell surface with possible repetition of the process; and (*c*) nonspecific binding or attachment of the SILs to the cell surface. Cellular association of SM-SIL[αCD19] or SM-SIL[Fab′] with CD19$^+$ Namalwa cells was higher than that of antibody-free controls (SM-SL) at all PL concentrations (Fig. 1*A*). At a PL concentration of 0.4 mM, the total cell association for SM-SIL[αCD19] or SM-SIL[Fab′] was around 3-fold higher than that for SM-SL ($P < 0.05$). HSPC-SIL[αCD19] and HSPC-SIL[Fab′] also had approximately 3-fold higher binding levels compared with HSPC-SL (data not shown). In addition, cellular association of SM-SIL[αCD19] and SM-SIL[Fab′] with cells at 37°C was significantly higher than that at 4°C (nonpermissive for endocytosis), suggesting a requirement for metabolic processes in the uptake of these immunoliposomes (Fig. 1*A*). SM-SIL[Fab′] had a higher level of association with the Namalwa cells than

[1] G. Charrois and T. M. Allen, Drug release rate influences the pharmacokinetics, biodistribution, therapeutic activity, and toxicity of pegylated liposomal doxorubicin formulations in murine breast cancer, submitted.

[2] P. Sapra, Antibody-targeted liposomal anticancer drugs (Thesis). Edmonton, AL: University of Alberta, 2003.

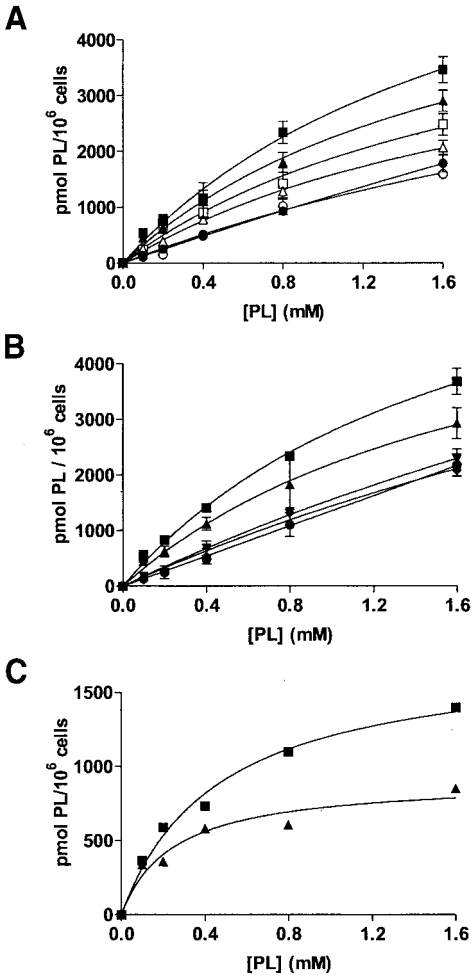

Fig. 1 *In vitro* cellular association of liposomes to Namalwa cells. Liposomes were labeled with cholesterol-[1,2-^{3}H-(*N*)]hexadecyl ether and incubated with 10^6 Namalwa cells, after which the cells were washed with cold PBS to remove the unbound liposomes. The concentration of monoclonal antibody (mAb) on SIL[αCD19] was 0.53–0.66 nmol binding domains of αCD19/μmol phospholipid (PL), whereas the concentration of Fab′ fragments on SIL[Fab′] was 0.36–0.45 nmol binding domains of Fab′/μmol PL. Data are expressed as pmol PL/10^6 cells. Each point is an average of three replicates ± SD, from one representative experiment. *A*, total cellular association of liposomes with cells as a function of concentration at 37°C (*closed symbols*) or 4°C (*open symbols*). SM-SL, (●, ○); SM-SIL[αCD19], (▲, △); SM-SIL-[Fab′], (■, □). *B*, total cellular association of liposomes with cells at 37°C compared with control liposomes targeted with nonspecific isotype-matched control mAb anti-PK136. SM-SL, (●); SM-SIL[αCD19], (▲); SM-SIL[Fab′], (■); SM-SIL[NS-Ab], (◆); SM-SIL[NS-Fab′], (▼). *C*, specific binding of SM-SIL[αCD19], (▲) or SM-SIL[Fab′], (■) with Namalwa cells.

SM-SIL[αCD19], although the total number of binding domains on the Fab′-coupled liposomes was actually lower than that on the IgG2a-coupled liposomes (Fig. 1*A*).

Nonspecific cellular association was determined by using radiolabeled liposomes coupled to an isotype-matched control antibody (anti-PK136) or its Fab′ fragments. Nonspecific association of anti-PK136-coupled liposomes with Namalwa cells increased linearly with increasing PL concentration (Fig. 1*B*) and was very similar to that observed for the nontargeted liposomes (SM-SL) shown in Fig. 1*A*. Specific cell association was determined by subtracting nonspecific association from the total cell association (Fig. 1*C*). The B_{max} was found to be 910 ± 100 pmol/10^6 cells for SM-SIL[αCD19] and 1760 ± 130 pmol/10^6 cells for SM-SIL[Fab′CD19] ($P < 0.005$). Also, there was a significant difference ($P < 0.05$) in K_d values between SM-SIL[αCD19] (250 ± 90 μM) and SM-SIL[Fab′CD19] (460 ± 80 μM).

***In Vitro* Cytotoxicity.** The *in vitro* cytotoxicities of various drug-loaded liposome formulations were determined for either 1- or 24-h incubations (Table 1). Cytotoxicity results, particularly at longer incubation times, are due to a combination of receptor binding and internalization of the encapsulated drug and uptake of the drug as free drug after its release (leakage) from the liposomes in the incubation media. The αCD19-targeted liposomal VCR formulations, *i.e.*, VCR-SM-SIL[αCD19] or VCR-SM-SIL[Fab′], displayed 23–28-fold higher cytotoxicity than the nontargeted formulations (VCR-SM-SL; $P < 0.005$) for 1-h incubations (Table 1). At the longer time point (24 h), no significant difference between targeted and nontargeted formulations was observed ($P > 0.05$). The cytotoxicity of VCR-SM-SIL[αCD19] was not significantly different from that of VCR-SM-SIL[Fab′] for either 1- or 24-h incubations ($P > 0.05$). In

Table 1 Cytotoxicity against Namalwa cells for liposomal formulations of vincristine (VCR) and doxorubicin (DXR) formulations and their respective free drugs

Formulation[a]	IC_{50}[b] (nM) VCR, 1 h	VCR, 24 h	DXR, 1 h × 10^{-3}
Free drug	39 ± 19	4.4 ± 1.1	1.5 ± 0.9
SL (nontargeted)	1070 ± 400	5.8 ± 2.2	>350
SIL[αCD19]	46 ± 10	3.9 ± 1.4	32 ± 9
SIL[Fab′]	37 ± 12	5.1 ± 4.2	34 ± 4
SIL[NS-Ab]	610 ± 370	6.4 ± 2.5	Not determined[c]
SIL[NS-Fab′]	400 ± 260	2.6 ± 2.0	Not determined[c]

[a] The VCR-containing liposomes were composed of egg sphingomyelin:cholesterol:methoxypoly(ethylene glycol) (M_r 2000) covalently linked via a carbamate bond to distearoylphosphatidylethanolamine (55:40:5) or egg sphingomyelin:cholesterol:methoxypoly(ethylene glycol) (M_r 2000) covalently linked via a carbamate bond to distearoylphosphatidylethanolamine:maleimide-derivatized poly(ethylene glycol)$_{2000}$-distearoylphosphatidylethanolamine (55:40:4:1), with 0.6–0.8 nmol binding domains of αCD19/μmol phospholipid or 0.45–0.64 nmol Fab′/μmol phospholipid. The DXR-containing liposomes were composed of hydrogenated soy phosphatidylcholine:cholesterol:methoxypoly(ethylene glycol) (M_r 2000), covalently linked via a carbamate bond to distearoylphosphatidylethanolamine (2:1:0.1) or hydrogenated soy phosphatidylcholine:cholesterol:methoxypoly(ethylene glycol) (M_r 2000), covalently linked via a carbamate bond to distearoylphosphatidylethanolamine:maleimide-derivatized poly(ethylene glycol)$_{2000}$-distearoylphosphatidylethanolamine (2:1:0.08:0.02) with 0.4 nmol binding domains of αCD19/μmol phospholipid or 0.39 nmol Fab′/μmol phospholipid.

[b] Drug concentration responsible for 50% growth inhibition in 3-(4,5-dimethylthiazol-2-yl)-2,5-diphenyltetrazolium bromide assay (see "Materials and Methods"), calculated with data from three to five separate experiments.

[c] DXR-containing formulations targeted with NS-Ab have been previously shown to be similar to DXR-SL (7).

addition, the cytotoxicity of targeted formulations approached that of free drug ($P > 0.05$). The IC_{50} values for formulations coupled to the isotype-matched antibody, *i.e.*, VCR-SM-SIL[NS-Ab] or VCR-SM-SIL[NS-Fab′], were significantly higher than those obtained for VCR-SM-SIL[αCD19] ($P < 0.05$) or VCR-SM-SIL[Fab′] ($P < 0.05$) and were not different from that of VCR-SM-SL ($P > 0.05$) for 1-h incubations.

Because cytotoxicity studies with DXR-loaded immunoliposomes have been reported previously (7), the current experiments comparing whole mAb with Fab′ were done only for a 1-h incubation time and demonstrated that the IC_{50} values for DXR-HSPC-SIL[Fab′] and DXR-HSPC-SIL[αCD19] were similar (Table 1). IC_{50} values for both types of targeted liposomes were lower than that obtained for nontargeted liposomes (DXR-HSPC-SL) but higher than the values obtained for free DXR.

Drug Release, Pharmacokinetics, and Biodistribution. The leakage of VCR was determined in 50% ABS at 37°C from targeted or nontargeted liposomes. SM-containing formulations of VCR are known to have significantly higher VCR leakage rates than that seen for leakage of DXR from DXR-HSPC-SL or DXR-HSPC-SIL (14, 35). The PL concentration of all of the formulations was 0.5 mM. The rate of leakage of VCR from VCR-SM-SIL[αCD19] ($t_{1/2} = 6.8 \pm 0.2$ h) was found to be similar to that for VCR-SM-SL ($t_{1/2} = 7.2 \pm 1.8$ h), indicating that the presence of the mAb did not affect drug release rates. In previous experiments, we have found that the $t_{1/2}$ for release of DXR from DXR-HSPC-SL is approximately 90 h.[1]

The pharmacokinetics and biodistribution of either nontargeted or targeted liposomes loaded with either VCR or DXR were examined in naïve BALB/c mice (Figs. 2 and 3). SIL[αCD19] were cleared more rapidly from the circulation than SIL[Fab′]; the latter demonstrated a pharmacokinetic profile that was very similar to nontargeted sterically stabilized (Stealth) liposomes (Fig. 2, *C* and *D*). For both VCR-loaded and DXR-loaded SIL formulations, the uptake of SIL[αCD19] into liver and spleen was significantly higher than that of SIL[Fab′] ($P < 0.001$) at all time points, likely due to Fc receptor-mediated mechanisms (Fig. 3).

VCR had faster drug release rates from the liposomes than DXR, as seen from lower plasma drug levels (Fig. 2, *A* and *B*) and the lower drug:lipid ratios (Fig. 2, *E* and *F*). The removal of the liposomal lipid (liposomes) from circulation was similar for both formulations (Fig. 2, *C* and *D*). In other words, for the VCR-containing formulations, at the longer time points, some drug-depleted liposomes were present in plasma.

Using the aqueous space marker ^{125}I-tyraminylinulin, the pharmacokinetics of the liposomes was also determined in tumor-bearing SCID mice at 24 h after i.v. inoculation of 5×10^6 Namalwa cells, and the results were similar to those found in naïve mice (data not shown). In tumor-bearing SCID mice, the blood levels for SM-SIL[Fab′] were not significantly different from those of SM-SL at 2 (87.2% and 84.9% of injected cpm, respectively) and 24 h (33.2% and 36.5%, respectively) postinjection. SM-SIL[αCD19], on the other hand, were rapidly cleared from the circulation. At 2 and 24 h, only 44.2% and 12.9%, respectively, of SM-SIL[αCD19] were still in the circulation in SCID mice ($P < 0.05$ compared with SM-SIL[Fab′]).

***In Vivo* Survival Experiments in Xenograft Models of Human B Lymphoma.** Fig. 4 gives the Kaplan-Meier plot for tumor-bearing mice treated with single injections of either free drug or liposomal formulations of either VCR or DXR. All treatments except free DXR significantly increased the survival of mice compared with controls ($P < 0.05$). DXR-HSPC-SL resulted in higher survival times than free DXR ($P < 0.05$), but VCR-SM-SL resulted in similar survival times to free VCR ($P > 0.05$). Both VCR-SM-SIL[αCD19] and VCR-SM-SIL-[Fab′], given at a dose of 0.66 mg/kg (*i.e.*, one-third of the MTD of 2 mg/kg), increased the survival of mice significantly compared with VCR-SM-SL ($P < 0.005$) or free VCR ($P < 0.05$), and both treatments resulted in long-term survivors. Mice receiving either DXR-HSPC-SIL[Fab′] or DXR-HSPC-SIL[αCD19] at the MTD for DXR (3 mg/kg in SCID mice) exhibited significantly increased survival times compared with either free DXR ($P < 0.005$) or DXR-HSPC-SL ($P < 0.005$). Mice treated with DXR-HSPC-SIL[Fab′] had significantly increased survival times compared with those receiving DXR-HSPC-SIL[αCD19] ($P < 0.005$). However, mice injected with VCR-SM-SIL[αCD19] appeared to have improved survival times compared with mice injected with VCR-SM-SIL[Fab′], but the differences did not reach statistical significance ($P > 0.05$). Also, the results achieved with VCR-SM-SIL[αCD19] and VCR-SM-SIL[Fab′] were superior to those obtained with their DXR-containing counterparts, despite the lower dose of VCR (0.66 mg/kg) relative to its MTD in SCID mice.

A separate therapeutic study was undertaken to examine whether αCD19 mAb or its Fab′ fragments had cytotoxic effects by themselves, when presented in association with drug-free liposomes. Mice injected with drug-free liposomes conjugated to Fab′ fragments (SM-SIL[Fab′]) had survival times that were the same as controls, whereas mice injected with drug-free liposomes conjugated to whole antibody (SM-SIL[αCD19]) had modestly increased survival times (30 days *versus* 27 days; results not shown). This suggests that αCD19 coupled to liposomes had, at the concentrations tested, some cytotoxic effects, probably through Fc-mediated complement-dependent cytotoxicity and/or antibody-dependent cell-mediated cytotoxicity mechanisms.

DISCUSSION

This study compares, for the first time, the binding, cytotoxicity, pharmacokinetics, and therapeutic outcomes in the same model system for immunoliposomal formulations of two different anticancer drugs, VCR and DXR. These drugs work via different mechanisms of action, have different physical and chemical properties and other drug-related properties such as mechanisms of resistance, and have different release rates from the liposomes. The study also compares the results for immunoliposomes targeted via αCD19 whole mAb compared with those targeted with Fab′ fragments. Although other investigators have shown the pharmacokinetic superiority of Fab′ fragments over whole mAbs as targeting agents (6, 34), our study is the first to directly compare the therapeutic effects of the two and to demonstrate that, for DXR-containing SIL[αCD19], pharmacokinetic superiority led to improved therapeutic results.

The Mal-PEG-DSPE coupling method results in a random

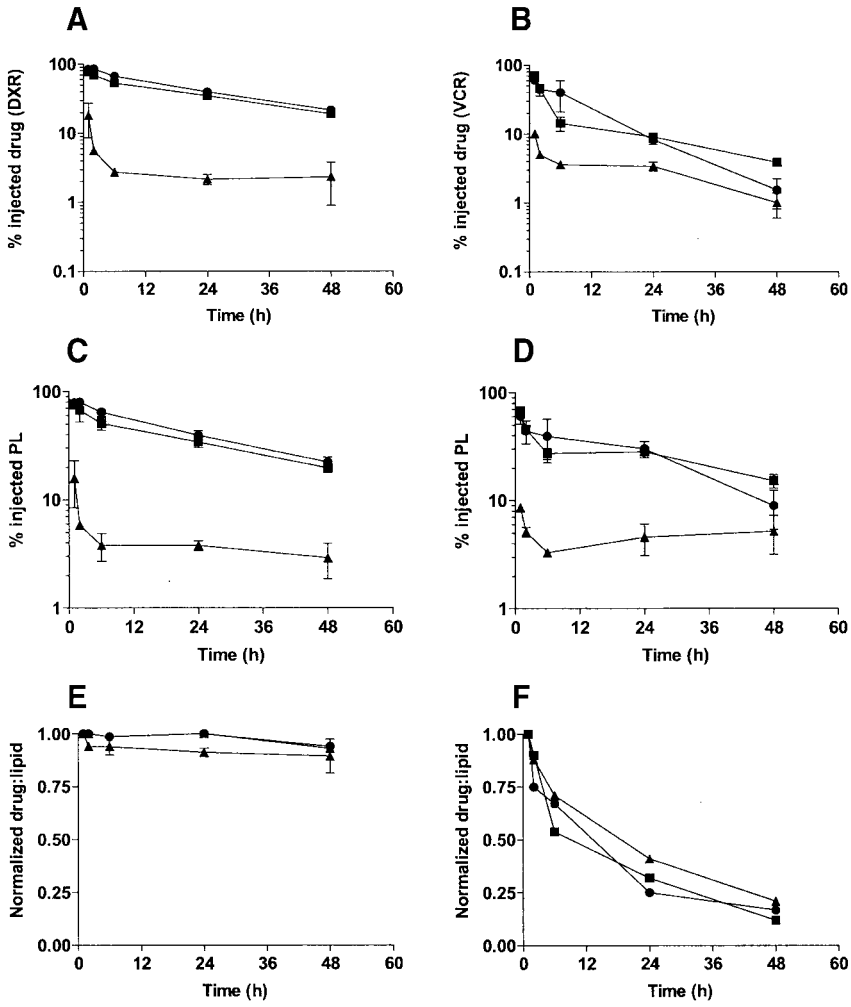

Fig. 2 Blood clearance of targeted *versus* nontargeted liposomes containing either radiolabeled doxorubicin (DXR) or vincristine (VCR) in naive BALB/c mice. Nontargeted liposomes loaded with VCR were composed of egg sphingomyelin (SM):cholesterol (Chol):methoxypoly(ethylene glycol) (M_r 2000), covalently linked via a carbamate bond to distearoylphosphatidylethanolamine (mPEG-DSPE; 55:40:5). Targeted liposomes loaded with VCR were composed of SM:Chol:mPEG-DSPE:maleimide-derivatized poly(ethylene glycol)$_{2000}$- distearoylphosphatidylethanolamine (Mal-PEG-DSPE; 55:40:4:1) and had 0.93 nmol binding domains of αCD19/μmol phospholipid (PL) or 1.07 nmol Fab′/μmol PL. Nontargeted liposomes loaded with DXR were composed of hydrogenated soy phosphatidylcholine (HSPC):Chol:mPEG-DSPE (2:1:0.1). Targeted liposomes loaded with DXR were composed of HSPC:Chol:mPEG-DSPE:Mal-PEG-DSPE (2:1:0.08:0.02) and had 1.3 nmol binding domains of αCD19/μmol PL or 1.6 nmol Fab′/μmol PL. Liposomes were radiolabeled with Chol-[1,2-^{3}H-(*N*)]hexadecyl ether and loaded with either [^{14}C]VCR or [^{14}C]DXR. Naïve BALB/c mice (3 mice/time point) received i.v. injection with a single bolus dose of 0.66 mg/kg liposomal VCR or 3 mg/kg liposomal DXR. At selected time points, mice were euthanized, and blood, liver, and spleen samples were analyzed for radioactivity. Data represent the mean ± SD of the percentage of injected drug (*A* and *B*, DXR and VCR, respectively) or PL (*C* and *D*, DXR or VCR, respectively) in blood ($n = 3$). *E* and *F* give the drug:lipid ratios for DXR- or VCR-containing liposomes, respectively, normalized to 1 at the time of injection. Sterically stabilized (Stealth) liposomes, (●); SIL[αCD19], (▲); SIL[Fab′], (■).

thiolation of the antibody molecules at the liposome surface, which leads to enhanced uptake of SIL[αCD19] by liver, spleen, and other macrophages via Fc receptor-mediated mechanisms. Using the thiol groups in the hinge region of Fab′ fragments to couple them to liposomes avoids three problems: (*a*) loss of antibody activity due to the potential thiolation of the antibody in the binding region; (*b*) decreased binding and/or increased clearance of the SILs due to random thiolation of the antibodies, which leads to random orientation of the antibodies and exposure of Fc domains at the liposome surface; and (*c*) the potential for cross-linking of either the antibodies or the liposomes. Coupling methods that prevent exposure of the Fc region (using the hydrazide-PEG-DSPE coupling method or coupling of Fab′ rather than whole mAbs) result in immunoliposomes that have clearance rates more similar to those of nontargeted liposomes (6, 7). Because therapeutic outcomes are correlated with increased circulation times, strategies that result in decreased clearance of liposomes have been predicted to result in increased survival times (29). However, one may lose antibody avidity by coupling to liposomes Fab′, with only one antigen

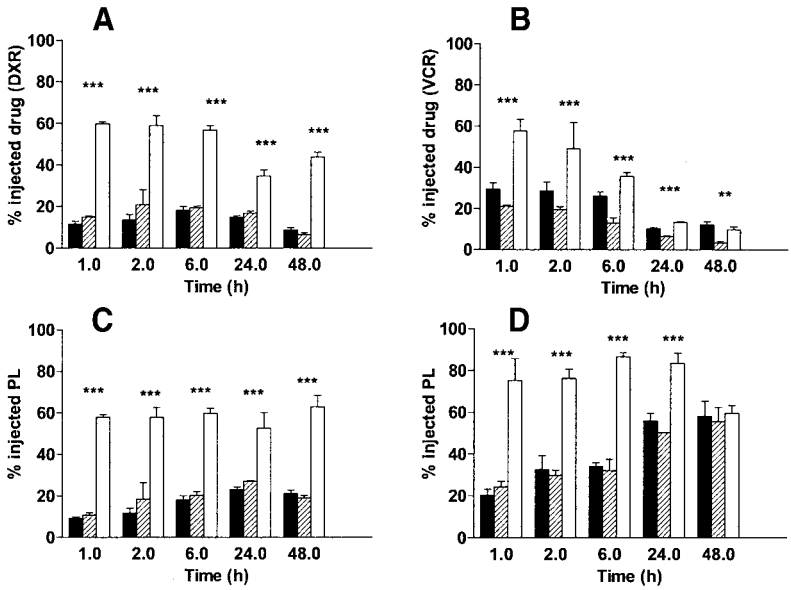

Fig. 3 Biodistribution of doxorubicin (DXR)- or vincristine (VCR)-loaded liposomes to mononuclear phagocyte system organs (liver + spleen) in naïve BALB/c mice. Nontargeted liposomes loaded with VCR were composed of egg sphingomyelin (SM):cholesterol (Chol):methoxypoly(ethylene glycol) (M_r 2000), covalently linked via a carbamate bond to distearoylphosphatidylethanolamine (mPEG-DSPE) [55:40:5 (mol/mol)]. Targeted liposomes loaded with VCR were composed of SM:Chol:mPEG-DSPE:maleimide-derivatized poly(ethylene glycol)$_{2000}$-distearoylphosphatidylethanolamine (Mal-PEG-DSPE) [55:40:4:1 (mol/mol)] and had 0.93 nmol binding domains of αCD19/μmol phospholipid (PL) or 1.1 nmol Fab′/μmol PL. Nontargeted liposomes loaded with DXR were composed of hydrogenated soy phosphatidylcholine (HSPC):Chol:mPEG-DSPE (2:1:0.1). Targeted liposomes loaded with DXR were composed of HSPC:Chol:mPEG-DSPE:Mal-PEG-DSPE (2:1:0.08:0.02) and had 1.3 nmol binding domains of αCD19/μmol PL or 1.6 nmol Fab′/μmol PL. Liposomes were radiolabeled with Chol-[1,2-^{3}H-(*N*)]hexadecyl ether and loaded with either [^{14}C]VCR or [^{14}C]DXR. Naïve BALB/c mice (3 mice/time point) received i.v. injection with a single bolus dose of 0.66 mg/kg liposomal VCR or 3 mg/kg liposomal DXR. At selected time points, mice were euthanized, and blood, liver, and spleen samples were analyzed for radioactivity. Data represent the mean ± SD of the percentage of injected drug (*A* and *B*, DXR and VCR, respectively) or PL (*C* and *D*, DXR or VCR, respectively) in the mononuclear phagocyte system (liver + spleen; $n = 3$). Sterically stabilized (Stealth) liposomes (SL), ■; SIL[αCD19], □; SIL[Fab′], ▨. **, $P < 0.01$; ***, $P < 0.001$ ($n = 3$).

binding domain, instead of whole mAbs, with two binding domains. Because the binding of the SIL[Fab′] was equivalent to or higher than that seen for SIL[αCD19], this suggests that coupling of Fab′ fragments to liposomes restores their avidity by restoring multivalent binding.

In the experiments where we demonstrated specific binding to CD19$^+$ human B lymphoma cells for targeted VCR and DXR formulations, every effort was made to ensure comparable number of antigen binding domains on the two types of formulations. The K_d values for SM-SIL[αCD19] were similar to those found for HSPC-SIL[αCD19] (7), suggesting that although liposome composition affects drug leakage rates (54), it does not affect the binding of the immunoliposomes to antigens at the cell surface.

We observed higher levels of cell association of both SM-SIL[αCD19] and SM-SIL[Fab′] to the Namalwa cells at 37°C compared with 4°C, where endocytosis does not occur. This is likely due to binding of the SILs to the cells via the pan B-cell differentiation antigen, CD19, followed by receptor-mediated endocytosis and recycling of the epitope back to the cell surface, where it will be available to partake in further binding and internalization events (7, 55–57). Confocal microscopy of fluorescent SIL[αCD19] shows fluorescence in the cytoplasm for Namalwa cells exposed to SIL[αCD19], but not for SIL[αCD20] (which is noninternalizing; Ref. 15).

After internalization of the liposomal drug packages, we have published evidence that the breakdown of the drug-liposome package by lysosomal and endosomal enzymes and release of drug into the cytoplasm are responsible for the cytotoxic effect produced by targeted liposomal DXR (14, 58, 59). This mechanism likely applies to the targeted liposomal VCR as well because both VCR-SM-SIL[αCD19] and VCR-SM-SIL[Fab′] demonstrated significantly higher cytotoxicity against the Namalwa cells than VCR-SM-SL after incubation for 1 h (Table 1). At shorter incubation times, release and uptake of the free drug into the cells is unlikely to play a major role in mediating cytotoxicity. For an incubation time of 24 h, a significant portion of the encapsulated drug would be released from VCR-containing liposomes and taken up into the cells as free drug. This explains why no significant differences were observed between targeted or nontargeted VCR-containing formulations and free drug at this time point. In the case of the DXR-loaded liposomes, the IC_{50} values of targeted liposomes were lower than for nontargeted liposomes after 24 h of incubation (7), which can be explained by the significantly slower rate of leakage of DXR from liposomes composed of HSPC:Chol:PEG (14).[1]

We performed therapeutic studies in a xenograft model of human B-cell lymphoma at a VCR dose that approximates the clinical dose in humans (one-third of the MTD in mice) and at

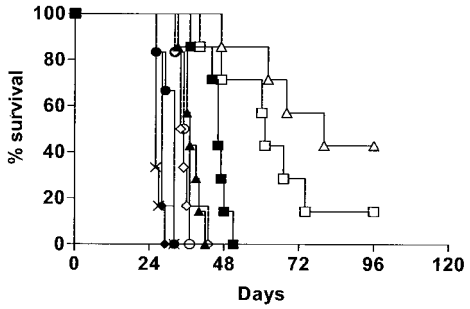

Fig. 4 Therapeutic efficacy of free drugs or liposomal formulations of drugs in severe combined immunodeficient mice injected with Namalwa cells. Severe combined immunodeficient mice (6–7 mice/group) received i.v. injection with 5×10^6 Namalwa cells in 0.2 ml of PBS, 24 h before i.v. treatment with a single bolus dose of free or liposomal drugs. Nontargeted liposomes loaded with vincristine (VCR) were composed of egg sphingomyelin (SM):cholesterol (Chol):methoxypoly(ethylene glycol) (M_r 2000), covalently linked via a carbamate bond to distearoylphosphatidylethanolamine (mPEG-DSPE) [55:40:5]. Targeted liposomes loaded with VCR were composed of SM:Chol:mPEG-DSPE: maleimide-derivatized poly(ethylene glycol)$_{2000}$-distearoylphosphatidylethanolamine (Mal-PEG-DSPE) [55:40:4:1] and had 0.82 nmol binding domains of αCD19/μmol phospholipid (PL) or 0.89 nmol Fab′/μmol PL. Nontargeted liposomes loaded with doxorubicin (DXR) were composed of hydrogenated soy phosphatidylcholine (HSPC):Chol: mPEG-DSPE (2:1:0.1). Targeted liposomes loaded with DXR were composed of HSPC:Chol:mPEG-DSPE:Mal-PEG-DSPE (2:1:0.08:0.02) and had 0.74 nmol binding domains of αCD19/μmol PL or 0.76 nmol Fab′/μmol PL. Free VCR or liposomal VCR was administered at a dose of 0.66 mg/kg, and free DXR or liposomal DXR was administered at a dose of 3 mg/kg. Saline control, (×) ; free VCR, (◇); VCR-SM-SL, (○); VCR-SM-SIL[αCD19], (△); VCR-SM-SIL[Fab′], (□); free DXR, (◆); DXR-HSPC-SL, (●); DXR-HSPC-SIL[αCD19], (▲); DXR-HSPC-SIL-[Fab′], (■).

a DXR dose that is the MTD in SCID mice. Our therapeutic results demonstrated that targeted liposomal formulations, containing either VCR or DXR, were superior to nontargeted liposomal drugs or to the free drugs, even though the SIL[αCD19] were cleared faster than the nontargeted liposomes. Because binding and internalization of αCD19 is a rapid process, our results suggest that SIL[αCD19] bound to and were internalized by the target cells more rapidly than they were cleared from the circulation by the mononuclear phagocytic system. However, the longer circulation times and the improved antigen accessibility of the SIL[Fab′] probably played an important role in further improving the therapeutic outcomes in mice injected with DXR-HSPC-SIL[Fab′] over mice injected with DXR-HSPC-SIL[αCD19].

Two drawbacks of VCR-loaded liposomes in the past were their relatively fast rates of drug release and clearance from circulation (35). Insertion of PEG-DSPE conjugates onto the surface of VCR-loaded liposomes can increase the circulation time of these liposomes, but it also increases the drug leakage rate (54). As a result, PEG-containing liposomal VCR had no therapeutic advantages over those lacking PEG (54). Our experiments showed that linking antibodies to the PEG terminus of VCR-loaded liposomes significantly improved the therapeutic outcomes. This is likely because the targeted formulations could rapidly deliver their drug to the target cells, before their contents were released.

No significant difference was observed between VCR-SM-SIL[αCD19] and VCR-SM-SIL[Fab′], unlike the superior performance of DXR-HSPC-SIL[Fab′] over DXR-HSPC-SIL[αCD19]. An explanation for the different results for DXR *versus* VCR may lie in the different release rates for the two drugs. The rate of release of VCR from the liposomes is fast relative to their rate of removal from the circulation into the mononuclear phagocytic system. Therefore, increasing the circulation times of VCR-containing liposomes would result in significantly more drug-depleted liposomes (*i.e.*, more lipid) being delivered to the target cells but would not result in the delivery of more drug. In other words, delivering drug-depleted liposomes to the cells is not expected to have a therapeutic advantage. On the other hand, for DXR-loaded immunoliposomes, which release their drug slowly on the time scale of plasma clearance, long circulation times would be expected to increase the amount of drug delivered to the target cells over time. Although mice injected with VCR-SM-SIL[αCD19] appeared to have improved survival times compared with mice injected with VCR-SM-SIL[Fab′], no statistical difference between the two groups was observed. The better results observed for VCR-SM-SIL[αCD19] may be due to synergy between cytotoxic effects of VCR and effects due to Fc-mediated mechanisms of anti-CD19 (antibody-dependent cell-mediated cytotoxicity and complement-dependent cytotoxicity).

We observed that free VCR, the nontargeted formulations, and the targeted VCR-containing formulations resulted in better therapeutic responses than each of the corresponding DXR-containing formulations. It appears that Namalwa cells are more sensitive to VCR than to DXR. Treatment of the tumor-bearing mice with free VCR resulted in a significant increase in survival relative to untreated controls, but this was not observed for free DXR relative to controls. Indeed, free DXR has little or no effect in this lymphoma model.

A plausible explanation for the better therapeutic results with the VCR-containing formulations over the DXR-containing formulations may involve the differential rate of release from liposomes of VCR and DXR and their different mechanisms of action. These drugs are cell cycle dependent and cell cycle independent, respectively. VCR acts by destabilizing microtubules, resulting in arrest of cells in the metaphase. Because cancer cells are not normally synchronized with respect to the cell cycle, exposure of the cancer cells to intracellular concentrations of VCR for periods of time that are as long as or longer than the cell cycle would allow cells in different phases of cell cycle to enter metaphase and be susceptible to the action of the drug. If the intracellular rate of release of VCR from the targeted liposomes after receptor-mediated internalization of the drug package is on a time scale that is similar to or longer than the doubling time of the cells, then cells will be exposed to therapeutic concentrations of drug as they go through metaphase, and good levels of cytotoxicity will result. Both *in vitro* studies (60, 61) and clinical trials (62, 63) have established the correlation between increased duration of VCR exposure to neoplastic cells and improved responses. To date, no studies on the intracellular rate of release of targeted liposomal VCR have been published.

DXR, on the other hand, is not a cell cycle-specific drug. It acts by multiple mechanisms including inhibition of topoisomerase II resulting in DNA strand breaks, inhibition of DNA

and RNA polymerase, oxidative DNA damage, and increasing ceramide levels leading to apoptosis. Hence, we can hypothesize that the cytotoxicity of DXR would be highest if the drug were delivered rapidly and in high concentrations to the target cells. We have previously published data showing that the rate of intracellular release of DXR from internalized formulations of DXR-HSPC-SIL[αCD19] was very slow, with appearance of DXR in the nucleus of Namalwa cells taking from 24 to 48 h (14, 59). The slow rate of release of DXR from the targeted liposomes, both before and after endocytosis, means that there may be a delay in the attainment of cytotoxic intracellular levels of drug, resulting in delayed cell kill and in lower overall cytotoxicity. In support of this concept, we have previously shown that engineering the targeted liposomes for increased rates of intracellular release from endosomes leads to increased cytotoxicities of liposomal formulations of DXR (58, 59). Additional experiments comparing immunoliposomal formulations of drugs with different release rates of DXR and VCR will help to refine this interpretation. In addition, the therapeutic effects of targeted formulations of other schedule-dependent drugs such as 5-fluorouracil, methotrexate, and topotecan could be compared with those of other schedule-independent drugs such as cisplatin and daunorubicin to examine whether schedule-specific effects play a role in the therapeutic results for liposomal drugs.

Besides acting via different mechanisms of action, VCR and DXR have other differences in drug-related properties such as mechanisms of drug resistance, potencies, and other physical and chemical properties. Any of these factors could be responsible, in part, for the improved therapeutics observed for VCR-containing immunoliposomes over DXR-containing immunoliposomes.

This study has shown excellent therapeutic results, particularly for αCD19-targeted formulations of VCR, in the treatment of a B-cell malignancy where the target cells either reside in the vasculature or appear to be readily accessible from the vasculature. Our responses to both drugs in this hematological model are significantly improved over responses achieved in several solid tumor models in our laboratory (64–66), where the "binding site barrier" (67) or Fc receptor-mediated endocytosis of the targeted liposomes by tumor macrophages may retard the diffusion of immunoliposomes through the tumor and limit their therapeutic effects. This suggests that other vasculature targets, *e.g.*, those specific to tumor vasculature, should be examined for their response to targeted liposomal drugs.

In conclusion, we have demonstrated that antibody-mediated targeting of VCR- or DXR-loaded liposomes to an internalizing epitope is a promising approach for the treatment of B-cell malignancies. We anticipate that the use of murine antibody Fab′ fragments or even smaller scFv fragments or the use of fully human antibody fragments as liposomal targeting moieties will decrease the incidence of human antimouse antibodies associated with the use of murine or chimeric antibodies and facilitate the progression of these formulations into clinical trials. The excellent results that we obtained in our human B lymphoma xenograft model for anti-CD19 Fab′-targeted formulations of liposomal VCR suggest that these formulations should receive clinical evaluation for the treatment of lymphoma or other B-cell malignancies.

ACKNOWLEDGMENTS

We acknowledge Inex Pharmaceuticals for expert advice regarding preparation of VCR liposomes and provision of radiolabeled VCR.

REFERENCES

1. Gabizon, A., and Papahadjopoulos, D. Liposome formulations with prolonged circulation time in blood and enhanced uptake by tumors. Proc. Natl. Acad. Sci. USA, *85:* 6949–6953, 1988.

2. Allen, T. M., Newman, M. S., Woodle, M. C., Mayhew, E., and Uster, P. S. Pharmacokinetics and anti-tumor activity of vincristine encapsulated in sterically stabilized liposomes. Int. J. Cancer, *62:* 199–204, 1995.

3. Ahmad, I., and Allen, T. M. Antibody-mediated specific binding and cytotoxicity of liposome-entrapped doxorubicin to lung cancer cells *in vitro*. Cancer Res., *52:* 4817–4820, 1992.

4. Lee, R. J., and Low, P. S. Folate-mediated tumor cell targeting of liposome-entrapped doxorubicin *in vitro.* Biochim. Biophys. Acta, *1233:* 134–144, 1995.

5. Park, J. W., Hong, K., Kirpotin, D. B., Meyer, O., Papahadjopoulos, D., and Benz, C. C. Anti-HER2 immunoliposomes for targeted therapy of human tumors. Cancer Lett., *118:* 153–160, 1997.

6. Maruyama, K., Takahashi, N., Tagawa, T., Nagaike, K., and Iwatsuru, M. Immunoliposomes bearing polyethyleneglycol-coupled Fab′ fragment show prolonged circulation time and high extravasation into targeted solid tumors *in vivo.* FEBS Lett., *413:* 177–180, 1997.

7. Lopes de Menezes, D. E., Pilarski, L. M., and Allen, T. M. *In vitro* and *in vivo* targeting of immunoliposomal doxorubicin to human B-cell lymphoma. Cancer Res., *58:* 3320–3330, 1998.

8. Pagnan, G., Montaldo, P. G., Pastorino, F., Chiesa, L., Raffaghello, L., Kirchmeier, M., Allen, T. M., and Ponzoni, M. GD_2-mediated melanoma cell targeting and cytotoxicity of liposome-entrapped fenretinide. Int. J. Cancer, *81:* 268–274, 1999.

9. Sugano, M., Egilmez, N. K., Yokota, S. J., Chen, F. A., Harding, J., Huang, S. K., and Bankert, R. B. Antibody targeting of doxorubicin-loaded liposomes suppresses the growth and metastatic spread of established human lung tumor xenografts in severe combined immunodeficient mice. Cancer Res., *60:* 6942–6949, 2000.

10. Moreira, J. N., Hansen, C. B., Gaspar, R., and Allen, T. M. A growth factor antagonist as a targeting agent for sterically stabilized liposomes in human small cell lung cancer. Biochim. Biophys. Acta, *1514:* 303–317, 2001.

11. Park, J. W., Hong, K., Kirpotin, D. B., Colbern, G., Shalaby, R., Baselga, J., Shao, Y., Nielsen, U. B., Marks, J. D., Moore, D., Papahadjopoulos, D., and Benz, C. C. Anti-HER2 immunoliposomes: enhanced efficacy attributable to targeted delivery. Clin. Cancer Res., *8:* 1172–1181, 2002.

12. Allen, T. M. Ligand-targeted therapeutics in anticancer therapy. Nat. Rev. Cancer, *2:* 750–763, 2002.

13. Allen, T. M., and Moase, E. H. Therapeutic opportunities for targeted liposomal drug delivery. Adv. Drug Delivery Rev., *21:* 117–133, 1996.

14. Lopes de Menezes, D. E., Kirchmeier, M. J., Gagne, J-F., Pilarski, L. M., and Allen, T. M. Cellular trafficking and cytotoxicity of anti-CD19-targeted liposomal doxorubicin in B lymphoma cells. J. Liposome Res., *9:* 199–228, 1999.

15. Sapra, P., and Allen, T. M. Internalizing antibodies are necessary for improved therapeutic efficacy of antibody-targeted liposomal drugs. Cancer Res., *62:* 7190–7194, 2002.

16. Pietras, R. J., Fendly, B. M., Chazin, V. R., and Pergram, M. D. Antibody to HER-2/neu receptor blocks DNA repair after cisplatin in human breast and ovarian cancer cells. Oncogene, *9:* 1829–1838, 1994.

17. Ghetie, M-A., Ghetie, V., and Vitetta, E. S. Anti-CD19 antibodies inhibit the function of the P-gp pump in multidrug-resistant B lymphoma cells. Clin. Cancer Res., *5:* 3920–3927, 1999.

18. Bradbury, L. E., Kansas, G. S., Levy, S., Evans, R. L., and Tedder, T. F. The CD19/CD21 signal transducing complex of human B-

lymphocytes includes the target of antiproliferative antibody-1 and leu-13 molecules. J. Immunol., *149:* 2841–2850, 1992.

19. Baselga, J., Norton, L., Albanell, J., Kim, Y. M., and Mendelsohn, J. Recombinant humanized anti-HER2 antibody (Herceptin) enhances the antitumor activity of paclitaxel and doxorubicin against HER2/neu-overexpressing human breast cancer xenografts. Cancer Res., *58:* 2825–2831, 1998.

20. Slamon, D. J., Leyland-Jones, B., Shak, S., Fuchs, H., Paton, V., Bajamonde, A., Fleming, T., Eiermann, W., Wolter, J., Pegram, M., Baselga, J., and Norton, L. Use of chemotherapy plus a monoclonal antibody against HER2 for metastatic breast cancer that overexpresses HER2. N. Engl. J. Med., *344:* 783–792, 2001.

21. Demidem, A., Lam, T., Alas, S., Hariharan, K., Hanna, N., and Bonavida, B. Chimeric anti-CD20 (IDEC-C2B8) monoclonal antibody sensitizes a B cell lymphoma cell line to cell killing by cytotoxic drugs. Cancer Biother. Radiopharm., *12:* 177–186, 1997.

22. Hansen, C. B., Kao, G. Y., Moase, E. H., Zalipsky, S., and Allen, T. M. Attachment of antibodies to sterically stabilized liposomes: evaluation, comparison and optimization of coupling procedures. Biochim. Biophys. Acta, *1239:* 133–144, 1995.

23. Schroff, R. W., Foon, K. A., Beatty, S. M., Oldham, R. K., and Morgan, A. C. Human anti-mouse immunoglobulin responses in patients receiving monoclonal antibody therapy. Cancer Res., *48:* 879–885, 1985.

24. Phillips, N. C., and Dahman, J. Immunogenicity of immunoliposomes: reactivity against species-specific IgG and liposomal phospholipids. Immunol. Lett., *45:* 149–152, 1995.

25. Carter, P. Improving the efficacy of antibody-based cancer therapies. Nat. Rev. Cancer, *1:* 118–129, 2001.

26. Aragnol, D., and Leserman, L. Immune clearance of liposomes inhibited by an anti-Fc receptor antibody *in vivo*. Proc. Natl. Acad. Sci. USA, *83:* 2699–2703, 1986.

27. Maruyama, K., Holmber, E., Kennel, S. J., Klibanov, A., Torchilin, V., and Huang, L. Characterization of *in vivo* immunoliposome targeting to pulmonary endothelium. J. Pharm. Sci., *79:* 978–984, 1990.

28. Harding, J. A., Engbers, C. M., Newman, M. S., Goldstein, N. I., and Zalipsky, S. Immunogenicity and pharmacokinetic attributes of poly(ethyleneglycol)-grafted immunoliposomes. Biochim. Biophys. Acta, *1327:* 181–192, 1997.

29. Papahadjopoulos, D., Allen, T. M., Gabizon, A., Mayhew, E., Matthay, K., Huang, S. K., Lee, K. D., Woodle, M. C., Lasic, D. D., Redemann, C., and Martin, F. J. Sterically stabilized liposomes: improvements in pharmacokinetics and antitumor therapeutic efficacy. Proc. Natl. Acad. Sci. USA, *88:* 11460–11464, 1991.

30. Huang, S. K., Lee, K. D., Hong, K., Friend, D. S., and Papahadjopoulos, D. Microscopic localization of sterically stabilized liposomes in colon carcinoma-bearing mice. Cancer Res., *52:* 5135–5143, 1992.

31. Scherphof, G. L., Kamps, J. A. A. M., and Koning, G. A. *In vivo* targeting of surface-modified liposomes to metastatically growing colon carcinoma cells and sinusoidal endothelial cells in the rat liver. J. Liposome Res., *7:* 419–432, 1997.

32. Martin, F. J., Hubbell, W. I., and Papahadjopoulos, D. Immunospecific targeting of liposomes to cells: a novel and efficient method for covalent attachment of Fab′ fragments via disulfide bonds. Biochemistry, *20:* 4229–4238, 1981.

33. Martin, F. J., and Papahadjopoulos, D. Irreversible coupling of immunoglobulin fragments to preformed vesicles. An improved method for liposome targeting. J. Biol. Chem., *257:* 286–288, 1982.

34. Pastorino, F., Brignole, C., Marimpietri, D., Sapra, P., Moase, E., Allen, T. M., and Ponzoni, M. Doxorubicin-loaded Fab′ fragments of anti-disialoganglioside immunoliposomes selectively inhibit the growth and dissemination of human neuroblastoma in nude mice. Cancer Res., *63:* 86–92, 2003.

35. Boman, N. L., Masin, D., Mayer, L. D., Cullis, P. R., and Bally, M. B. Liposomal vincristine which exhibits increased drug retention and increased circulation longevity cures mice bearing P388 tumors. Cancer Res., *54:* 2830–2833, 1994.

36. Gelmon, K. A., Tolcher, A., Diab, A. R., Bally, M. B., Embree, L., Hudon, N., Dedhar, C., Ayers, D., Eisen, A., Melosky, B., Burge, C., Logan, P., and Mayer, L. D. Phase I study of liposomal vincristine. J. Clin. Oncol., *17:* 697–705, 1999.

37. Sarris, A. H., Hagemeister, F., Romanguera, J., Rodriguez, M. A., McLaughlin, P., Tsimberidou, A. M., Medeiros, L. J., Samuels, B., Pate, O., Oholendt, M., Kantarjian, H., Burge, C., and Cabanillas, F. Liposomal vinicristine in relapsed non-Hodgkin's lymphomas: early results of an ongoing Phase II trial. Ann. Oncol., *11:* 69–72, 2000.

38. Northfelt, D. W., Dezube, B. J., Thommes, J. A., Levine, R., Von Roenn, J. H., Dosik, G. M., Rios, A., Krown, S. E., DuMond, C., and Mamelok, R. D. Efficacy of pegylated-liposomal doxorubicin in the treatment of AIDS-related Kaposi's sarcoma after failure of standard chemotherapy. J. Clin. Oncol., *15:* 653–659, 1997.

39. Muggia, F., Hainsworth, J. D., Jeffers, S., Miller, P., Groshen, S., Tan, M., Roman, L., Uziely, B., Muderspach, L., Garcia, A., Burnett, A., Greco, F. A., Morrow, C. P., Paradiso, L. J., and Liang, L-J. Phase II study of liposomal doxorubicin in refractory ovarian cancer: antitumor activity and toxicity modification by liposomal encapsulation. J. Clin. Oncol., *15:* 987–993, 1997.

40. Safra, T., Muggia, F., Jeffers, S., Tsao-Wei, D. D., Groshen, S., Lyass, O., Henderson, R., Berry, G., and Gabizon, A. Pegylated liposomal doxorubicin (Doxil): reduced clinical cardiotoxicity in patients reaching or exceeding cumulative doses of 500 mg/m^2. Ann. Oncol., *11:* 1029–1033, 2000.

41. Lopes de Menezes, D. E., Pilarski, L. M., Belch, A. R., and Allen, T. M. Selective targeting of immunoliposomal doxorubicin against human multiple myeloma *in vitro* and *ex vivo*. Biochim. Biophys. Acta, *1466:* 205–220, 2000.

42. Allen, T. M., Hansen, C. B., Martin, F., Redemann, C., and Yau-Young, A. Liposomes containing synthetic lipid derivatives of poly(ethylene glycol) show prolonged circulation half-lives *in vivo*. Biochim. Biophys. Acta, *1066:* 29–36, 1991.

43. Kirpotin, D., Park, J. W., Hong, K., Zalipsky, S., Li, W-L., Carter, P., Benz, C. C., and Papahadjopoulos, D. Sterically stabilized anti-HER2 immunoliposomes: design and targeting to human breast cancer cells *in vitro*. Biochemistry, *36:* 66–75, 1997.

44. Zola, H., Macardle, P. J., Bradford, T., Weedon, H., Yasui, H., and Kurosawa, Y. Preparation and characterization of a chimeric CD19 monoclonal antibody. Immunol. Cell Biol., *69:* 411–422, 1991.

45. Iden, D. L., and Allen, T. M. *In vitro* and *in vivo* comparison of immunoliposomes made by conventional coupling techniques with those made by a new post-insertion technique. Biochim. Biophys. Acta, *1513:* 207–216, 2001.

46. Yamaguchi, Y., Kim, H., Kato, K., Masuda, K., Shimada, I., and Arata, Y. Proteolytic fragmentation with high specificity of mouse immunoglobulin G. J. Immunol. Methods, *181:* 259–267, 1995.

47. Mayer, L. D., Bally, M. B., Loughrey, H., Masin, D., and Cullis, P. R. Liposomal vincristine preparations which exhibit decreased drug toxicity and increased activity against murine L1210 and P388 tumors. Cancer Res., *50:* 575–579, 1990.

48. Bartlett, G. R. Phosphorus assay in column chromatography. J. Biol. Chem., *234:* 466–468, 1959.

49. Bolotin, E. M., Cohen, R., Bar, L. K., Emanuel, S. N., Lasic, D. D., and Barenholz, Y. Ammonium sulphate gradients for efficient and stable remote loading of amphipathic weak bases into liposomes and ligandosomes. J. Liposome Res., *4:* 455–479, 1994.

50. Harasym, T. O., Cullis, P. R., and Balley, M. B. Intratumor distribution of doxorubicin following i.v. administration of drug encapsulated in egg phosphaticdylcholine/cholesterol liposomes. Cancer Chemother. Pharmacol., *40:* 309–317, 1997.

51. Parr, M. J., Masin, D., Cullis, P. R., and Bally, M. B. Accumulation of liposomal lipid and encapsulated doxorubicin in murine Lewis lung carcinoma: the lack of beneficial effects by coating liposomes with poly(ethylene glycol). J. Pharmacol. Exp. Ther., *280:* 1319–1327, 1997.

52. Webb, M. S., Logan, P., Kanter, P. M., St.-Onge, G., Gelmon, K., Harasym, T., Mayer, L. D., and Bally, M. B. Preclinical pharmacology, toxicology and efficacy of sphingomyelin/cholesterol liposomal vincris-

tine for therapeutic treatment of cancer. Cancer Chemother. Pharmacol., *42:* 461–470, 1998.

53. Allen, T. M. Liposomes in the therapy of infectious diseases and cancer. *In:* UCLA Symposium on Molecular and Cellular Biology, pp. 405–415. New York: Alan R. Liss, 1988.

54. Webb, M. S., Harasym, T. O., Masin, D., Bally, M. B., and Mayer, L. D. Sphingomyelin cholesterol liposomes significantly enhance the pharmacokinetic and therapeutic properties of vincristine in murine and human tumour models. Br. J. Cancer, *72:* 896–904, 1995.

55. Uckun, F. M., Jaszcz, W., Ambrus, J. L., Fauci, A. S., Gajl-Peczalska, K., Song, S. W., Wick, M. R., Myers, D. E., Waddick, K., and Ledbetter, J. A. Detailed studies on expression and function of CD19 surface determinant by using B43 monoclonal antibody and the clinical potential of anti-CD19 immunotoxins. Blood, *71:* 13–29, 1988.

56. Press, O. W., Farr, A. G., Borroz, K. I., Andersen, S. K., and Martin, P. J. Endocytosis and degradation of monoclonal antibodies targeting human B-cell malignancies. Cancer Res., *49:* 4906–4912, 1989.

57. van Oosterhout, Y. V., van den Herik-Oudijk, I. E., Wessels, H. M., de Witte, T., van de Winkel, J. G., and Preijers, F. W. Effect of isotype on internalization and cytotoxicity of CD19-ricin A immunotoxins. Cancer Res., *54:* 3527–3532, 1994.

58. Ishida, T., Kirchmeier, M. J., Moase, E. H., Zalipsky, S., and Allen, T. M. Targeted delivery and triggered release of liposomal doxorubicin enhances cytotoxicity against human B lymphoma cells. Biochim. Biophys. Acta, *1515:* 144–158, 2001.

59. Kirchmeier, M. J., Ishida, T., Chevrette, J., and Allen, T. M. Correlations between the rate of intracellular release of endocytosed liposomal doxorubicin and cytotoxicity as determined by a new assay. J. Liposome Res., *11:* 15–29, 2001.

60. Jackson, D. V., Jr., and Bender, R. A. Cytotoxic thresholds of vincristine in a murine and a human leukemia cell line *in vitro.* Cancer Res., *39:* 4346–4349, 1979.

61. Mayer, L. D., Nayar, R., Thies, R. L., Boman, N. L., Cullis, P. R., and Bally, M. B. Identification of vesicle properties that enhance the antitumor activity of liposomal vincristine against murine L1210 leukemia. Cancer Chemother. Pharmacol., *33:* 17–24, 1993.

62. Jackson, D. V., Jr., Jobson, V. W., Homesley, H. D., Welander, C., Hire, E. A., Pavy, M. D., Votaw, M. L., Richards, F., II, and Muss, H. B. Vincristine infusion in refractory gynecologic malignancies. Gynecol. Oncol., *25:* 212–216, 1986.

63. Jackson, D. V., White, D. R., Spurr, C. L., Hire, E. A., Pavy, M. D., Robertson, M., Legos, H. C., and McMahan, R. A. Moderate-dose vincristine infusion in refractory breast cancer. Am. J. Clin. Oncol., *9:* 376–378, 1986.

64. Allen, T. M., Ahmad, I., Lopes de Menezes, D. E., and Moase, E. H. Immunoliposome-mediated targeting of anti-cancer drugs *in vivo*. Biochem. Soc. Trans., *23:* 1073–1079, 1995.

65. Moase, E., Qi, W., Ishida, T., Gabos, Z., Longenecker, B. M., Zimmermann, G. L., Ding, L., Krantz, M., and Allen, T. M. Anti-MUC-1 immunoliposomal doxorubicin in the treatment of murine models of metastatic breast cancer. Biochim. Biophys. Acta, *1510:* 43–55, 2001.

66. Moreira, J. N., Gaspar, R., and Allen, T. M. Targeting Stealth liposomes in a murine model of human small cell lung cancer. Biochim. Biophys. Acta, *1515:* 167–176, 2001.

67. Weinstein, J. N., and van Osdol, W. Early intervention in cancer using monoclonal antibodies and other biological ligands: micropharmacology and the "binding site barrier." Cancer Res., *52:* 2747–2751, 1992.